Towards jitter-free pump-probe measurements at seeded free electron laser facilities

Miltcho B. Danailov,[1,*] Filippo Bencivenga,[1] Flavio Capotondi,[1] Francesco Casolari,[1] Paolo Cinquegrana,[1] Alexander Demidovich,[1] Erika Giangrisostomi,[1] Maya P. Kiskinova,[1] Gabor Kurdi,[1] Michele Manfredda,[1] Claudio Masciovecchio,[1] Riccardo Mincigrucci,[1,2] Ivaylo P. Nikolov,[1] Emanuele Pedersoli,[1] Emiliano Principi,[1] and Paolo Sigalotti[1]

[1]*Elettra-Sincrotrone Trieste, SS 14 - km 163.5, 34149 Basovizza, Trieste, Italy*
[2]*Dipartimento di Fisica, Università di Perugia, Via A. Pascoli, 06123 Perugia, Italy*
[*]*danailovm@elettra.eu*

Abstract: X-ray free electron lasers (FEL) coupled with optical lasers have opened unprecedented opportunities for studying ultrafast dynamics in matter. The major challenge in pump-probe experiments using FEL and optical lasers is synchronizing the arrival time of the two pulses. Here we report a technique that benefits from the seeded-FEL scheme and uses the optical seed laser for nearly jitter-free pump-probe experiments. Timing jitter as small as 6 fs has been achieved and confirmed by measurements of FEL-induced transient reflectivity changes of Si_3N_4 using both collinear and non-collinear geometries. Planned improvements of the experimental set-up are expected to further reduce the timing jitter between the two pulses down to fs level.

OCIS codes: (140.2600) Free-electron lasers (FELs); (320.7120) Ultrafast phenomena; (320.7100) Ultrafast measurements; (320.7130) Ultrafast processes in condensed matter, including semiconductors.

References and links

1. P. Emma, R. Akre, J. Arthur, R. Bionta, C. Bostedt, J. Bozek, A. Brachmann, P. Bucksbaum, R. Coffee, F.-J. Decker, Y. Ding, D. Dowell, S. Edstrom, A. Fisher, J. Frisch, S. Gilevich, J. Hastings, G. Hays, Ph. Hering, Z. Huang, R. Iverson, H. Loos, M. Messerschmidt, A. Miahnahri, S. Moeller, H.-D. Nuhn, G. Pile, D. Ratner, J. Rzepiela, D. Schultz, T. Smith, P. Stefan, H. Tompkins, J. Turner, J. Welch, W. White, J. Wu, G. Yocky, and J. Galayda, "First lasing and operation of an ångstrom-wavelength free-electron laser," Nat. Photonics **4**(9), 641–647 (2010).
2. S. Tanaka and S. Mukamel, "X-ray four-wave mixing in molecules," J. Chem. Phys. **116**(5), 1877–1891 (2002).
3. F. Bencivenga, S. Baroni, C. Carbone, M. Chergui, M. B. Danailov, G. De Ninno, M. Kiskinova, L. Raimondi, C. Svetina, and C. Masciovecchio, "Nanoscale dynamics by short-wavelength four wave mixing experiments," New J. Phys. **15**(12), 123023 (2013).
4. M. Beye, O. Krupin, G. Hays, A. H. Reid, D. Rupp, S. de Jong, S. Lee, W.-S. Lee, Y.-D. Chuang, R. Coffee, J. P. Cryan, J. M. Glownia, A. Föhlisch, M. R. Holmes, A. R. Fry, W. E. White, C. Bostedt, A. O. Scherz, H. A. Durr, and W. F. Schlotter, "X-ray pulse preserving single-shot optical cross-correlation method for improved experimental temporal resolution," Appl. Phys. Lett. **100**(12), 121108 (2012).
5. E. S. Noël, M. Verhoeven, A. K. Lagendijk, F. Tessadori, K. Smith, S. Choorapoikayil, J. den Hertog, and J. Bakkers, "A nodal-independent and tissue-intrinsic mechanism controls heart-looping chirality," Nat. Commun. **4**, 2754 (2013).
6. Y. Obara, T. Katayama, Y. Ogi, T. Suzuki, N. Kurahashi, S. Karashima, Y. Chiba, Y. Isokawa, T. Togashi, Y. Inubushi, M. Yabashi, T. Suzuki, and K. Misawa, "Femtosecond time-resolved X-ray absorption spectroscopy of liquid using a hard X-ray free electron laser in a dual-beam dispersive detection method," Opt. Express **22**(1), 1105–1113 (2014).
7. S. Schulz, M. K. Czwalinna, M. Felber, P. Prędki, S. Schefer, H. Schlarb, and U. Wegner, "Femtosecond-precision synchronization of the pump-probe optical laser for user experiments at FLASH," Proc. SPIE **8778**, 87780R (2013).
8. P. Cinquegrana, S. Cleva, A. Demidovich, G. Gaio, R. Ivanov, G. Kurdi, I. Nikolov, P. Sigalotti, and M. B. Danailov, "Optical beam transport to remote location for low jitter pump-probe experiments with Free Electron Laser," Phys. Rev. ST Accel. Beams **17**(4), 040702 (2014).

#208592 - $15.00 USD Received 21 Mar 2014; revised 8 May 2014; accepted 8 May 2014; published 20 May 2014

9. L. H. Yu, "Generation of intense UV radiation by subharmonically seeded single-pass free-electron lasers," Phys. Rev. A **44**(8), 5178–5193 (1991).
10. E. Allaria, R. Appio, L. Badano, W. A. Barletta, S. Bassanese, S. G. Biedron, A. Borga, E. Busetto, D. Castronovo, P. Cinquegrana, S. Cleva, D. Cocco, M. Cornacchia, P. Craievich, I. Cudin, G. D'Auria, M. Dal Forno, M. B. Danailov, R. De Monte, G. De Ninno, P. Delgiusto, A. Demidovich, S. Di Mitri, B. Diviacco, A. Fabris, R. Fabris, W. Fawley, M. Ferianis, E. Ferrari, S. Ferry, L. Froehlich, P. Furlan, G. Gaio, F. Gelmetti, L. Giannessi, M. Giannini, R. Gobessi, R. Ivanov, E. Karantzoulis, M. Lonza, A. Lutman, B. Mahieu, M. Milloch, S. V. Milton, M. Musardo, I. Nikolov, S. Noe, F. Parmigiani, G. Penco, M. Petronio, L. Pivetta, M. Predonzani, F. Rossi, L. Rumiz, A. Salom, C. Scafuri, C. Serpico, P. Sigalotti, S. Spampinati, C. Spezzani, M. Svandrlik, C. Svetina, S. Tazzari, M. Trovo, R. Umer, A. Vascotto, M. Veronese, R. Visintini, M. Zaccaria, D. Zangrando, and M. Zangrando, "Highly coherent and stable pulses from the FERMI seeded free-electron laser in the extreme ultraviolet," Nat. Photonics **6**(10), 699–704 (2012).
11. E. Allaria, D. Castronovo, P. Cinquegrana, P. Craievich, M. Dal Forno, M. B. Danailov, G. D'Auria, A. Demidovich, G. De Ninno, S. Di Mitri, B. Diviacco, W. M. Fawley, M. Ferianis, E. Ferrari, L. Froehlich, G. Gaio, D. Gauthier, L. Giannessi, R. Ivanov, B. Mahieu, N. Mahne, I. Nikolov, F. Parmigiani, G. Penco, L. Raimondi, C. Scafuri, C. Serpico, P. Sigalotti, S. Spampinati, C. Spezzani, M. Svandrlik, C. Svetina, M. Trovo, M. Veronese, D. Zangrando, and M. Zangrando, "Two-stage seeded soft-X-ray free-electron laser," Nat. Photonics **7**(11), 913–918 (2013).
12. T. Togashi, E. J. Takahashi, K. Midorikawa, M. Aoyama, K. Yamakawa, T. Sato, A. Iwasaki, S. Owada, T. Okino, K. Yamanouchi, F. Kannari, A. Yagishita, H. Nakano, M. E. Couprie, K. Fukami, T. Hatsui, T. Hara, T. Kameshima, H. Kitamura, N. Kumagai, S. Matsubara, M. Nagasono, H. Ohashi, T. Ohshima, Y. Otake, T. Shintake, K. Tamasaku, H. Tanaka, T. Tanaka, K. Togawa, H. Tomizawa, T. Watanabe, M. Yabashi, and T. Ishikawa, "Extreme ultraviolet free electron laser seeded with high-order harmonic of Ti:sapphire laser," Opt. Express **19**(1), 317–324 (2011).
13. G. Stupakov, "Using the beam-echo effect for generation of short-wavelength radiation," Phys. Rev. Lett. **102**(7), 074801 (2009).
14. P. Sigalotti, P. Cinquegrana, A. Demidovich, R. Ivanov, I. Nikolov, G. Kurdi, and M. B. Danailov, "Ultrafast laser synchronization at the FERMI@ELETTRA FEL," Proc. SPIE **8778**, 87780Q (2013).
15. M. B. Danailov, P. Cinquegrana, A. Demidovich, R. Ivanov, I. Nikolov, and P. Sigalotti, "Design and first experience with the FERMI seed laser," in *Proceedings of the 33rd International Free Electron Laser Conference*, Z. Zhao and D. Wang, eds. (SINAP, Shanghai, 2011).
16. M. Harmand, R. Coffee, M. R. Bionta, M. Chollet, D. French, D. Zhu, D. M. Fritz, H. T. Lemke, N. Medvedev, B. Ziaja, S. Toleikis, and M. Cammarata, "Achieving few-femtosecond time-sorting at hard X-ray free-electron lasers," Nat. Photonics **7**(3), 215–218 (2013).
17. L. Raimondi, C. Svetina, N. Mahne, D. Cocco, A. Abrami, M. De Marco, C. Fava, S. Gerusina, R. Gobessi, F. Capotondi, E. Pedersoli, M. Kiskinova, G. De Ninno, P. Zeitoun, G. Dovillaire, G. Lambert, W. Boutu, H. Merdji, A. I. Gonzalez, D. Gauthier, and M. Zangrando, "Microfocusing of the FERMI@Elettra FEL beam with a K-B active optics system: spot size predictions by application of the WISE code," Nucl. Instrum. Methods A **710**, 131–138 (2013).
18. O. Krupin, M. Trigo, W. F. Schlotter, M. Beye, F. Sorgenfrei, J. J. Turner, D. A. Reis, N. Gerken, S. Lee, W. S. Lee, G. Hays, Y. Acremann, B. Abbey, R. Coffee, M. Messerschmidt, S. P. Hau-Riege, G. Lapertot, J. Lüning, P. Heimann, R. Soufli, M. Fernández-Perea, M. Rowen, M. Holmes, S. L. Molodtsov, A. Föhlisch, and W. Wurth, "Temporal cross-correlation of x-ray free electron and optical lasers using soft x-ray pulse induced transient reflectivity," Opt. Express **20**(10), 11396–11406 (2012).
19. S. M. Durbin, "X-ray induced optical reflectivity," AIP Adv. **2**(4), 042151 (2012).

1. Introduction

Free Electron Laser (FEL) technology is currently developing extremely fast and the possibility to have fully coherent pulses in the extreme ultraviolet (XUV) and soft x-ray photon energy range is becoming a reality [1–3].Using such wavelengths one can stimulate and probe electronic transitions from core levels, a revolutionary step in accessing ultrafast phenomena in matter on the nanoscale with chemical selectivity. As an example, it has been theoretically demonstrated that, using two different pulses, it is possible to coherently stimulate an exciton while being resonant with a core transition of a specific atomic site in the investigated system. Then the ultrafast evolution of such an exciton can be probed by a third pulse having photon energy tuned to a core transition of another selected atom, introducing in this way the highly desired chemical sensitivity in both the stimulation and probe processes [3]. This is an experiment that today many scientists are dreaming for.

Due to the ultrashort (femtosecond or sub-femtosecond) lifetime of core excitations, a necessary condition to carry out experiments, involving sample interaction with both FEL and external optical laser pulses, is the generation of FEL/external laser pulse pairs with timing

#208592 - $15.00 USD Received 21 Mar 2014; revised 8 May 2014; accepted 8 May 2014; published 20 May 2014

jitter down to the few fs level. Achieving such performance is a major challenge since the synchronization on the external laser with the FEL pulses involves a number of subsystems at separate locations. On one side a dedicated Photo Injector Laser (PIL) initiates the FEL process by generating an electron bunch, which is accelerated, compressed and propagated in a chain of undulators where the FEL pulses are emitted and then transported to the experimental stations. In the standard approach a time resolved experiments combines the FEL pulse with an external (IR, VIS or UV) laser pulse. The latter is generated by a dedicated User Laser (further referred to as USL), located close to the experimental stations, i.e. typically hundreds of meters away from the PIL. Even though the PIL and USL are synchronized to a common reference signal there are various noise sources affecting the complex chain involved in both the FEL and the external laser pulse generation. This leads to unavoidable accumulation of a synchronization error that typically exceeds 100 fs RMS at the existing FEL facilities [4–6]. The best result reported so far has recently been obtained at FLASH where the relative timing jitter between the FEL and external laser pulses was measured to be 33 fs RMS [7].

We have recently proposed and developed an alternative technique for obtaining an extremely low jitter between and external laser pulses and the pulses emitted by a seeded FEL [8]. In our scheme a portion of the seed laser is transported to the experimental stations and used for pump-probe experiments. Due to the intrinsic synchronization of the FEL pulse with the seed laser pulse, our approach eliminates the main sources contributing to timing jitter in the standard scheme, so only the beam transport of the seed laser (SL) pulse to the experimental stations remains a possible source of appreciable timing fluctuations. However, as it has been shown in Ref [8], over a distance of 150 m (typical for FEL facilities) a carefully designed optical beam transport allows to keep the added timing jitter to a sub-5 fs level. Here we report first transient reflectivity results obtained with this setup measured in two of the FERMI experimental stations. We demonstrate that the infrared laser and FEL pulses arrive at the sample with a relative timing jitter that can be as low as 6 fs and the timing drifts are negligible over tens of minutes. With relatively straightforward improvements, discussed at the end of the paper, the timing jitter between the FEL and laser pulse in our scheme can be pushed to the few fs level, opening unique opportunities for multi-pulse table-top laser type experiments with FELs.

2. Basic idea and scheme

First we briefly recall some FEL basics needed to understand the proposed scheme. Figure 1 shows a simplified sketch of typical short wavelength FEL facility. The FEL process is initiated by a UV pulse generated by the Photo Injector Laser and sent to a radiofrequency (RF) photoinjector, where an electron bunch of typical length of about 10 ps is generated. The bunch is accelerated in a Linear Accelerator (LINAC) to energy from 500 eV to several GeV (depending on the FEL wavelength range) and compressed to a few hundred fs in magnetic compression structures. The FEL process occurs in a chain of properly tuned undulators, where the bunch is sent after the compression. In the most popular, so called Self Amplified Spontaneous Emission (SASE) scheme, the FEL radiation starts from shot noise, generated by the accelerated electron bunch in the first undulator and the X-ray laser pulse is produced by amplification of this radiation in the following undulator chain. In the second, seeded FEL scheme, an external Seed Laser (SL) gives rise to highly coherent X-ray pulse. The pump-probe scheme described here has been implemented at the FERMI FEL. FERMI is based on the so called High Gain Harmonic Generation (HGHG) seeding [9] and uses high power seed pulses, which modulate the accelerated electron bunch in the first undulator. The bunch propagates further in a chain of undulators tuned at the desired harmonic of the seed laser wavelength and emits a highly coherent pulse at the X-ray wavelength [10,11]. It is important to stress that in the seeded scheme the exact time of emission of the FEL pulse is determined (with an accuracy of below 1 fs) by the temporal position of the seed pulse. This feature

#208592 - $15.00 USD Received 21 Mar 2014; revised 8 May 2014; accepted 8 May 2014; published 20 May 2014

remains true also for the other seeding techniques, like direct seeding [12] or echo-enhanced harmonic generation [13].

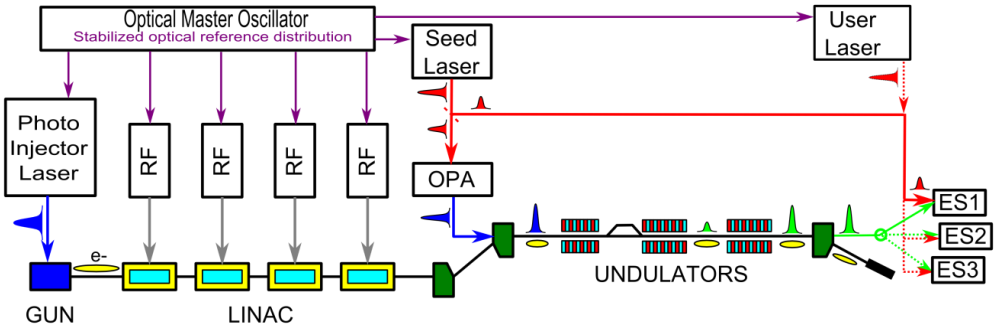

Fig. 1. General layout of an FEL facility, illustrating the standard approach (separate User Laser synchronized to the Optical Master Oscillator) and the proposed here approach (optically propagated fraction of the Seed Laser) to Pump-Probe experiments.

As mentioned above, when using an external laser pulse for pump-probe experiments it should arrive at the sample with a perfectly defined time delay (i.e. negligible timing jitter) with respect to the FEL pulse. The main sources of the FEL-to-external laser jitter are the synchronization of the ultrafast lasers (PIL and USL) to the reference signal, the acceleration process in the LINAC (e.g. noise in the RF given to the accelerating sections) and the noise affecting the distribution of the reference signal. Once the FEL process is initiated, the time-of-flight through the undulator chain and to the experimental chamber has negligible jitter and may only exhibit slow drifts due to temperature changes. The seeded FEL scheme exhibits intrinsically smaller jitter than the SASE FEL scheme because the seeding process cancels the timing jitter accumulated by the electron bunch. This may still be not sufficient, so we make a further step ahead allowing cancellation of additional jitter terms. As it can be seen from Fig. 1 this is obtained by using portions of the same laser pulse for FEL seed and for pump-probe experiments. The common infrared (IR) laser pulse is generated by a Ti:sapphire amplifier. One part of the IR beam is used to generate the seed by pumping an Optical Parametric Amplifier (OPA). The remaining part of the beam (shown in red) is sent through a dedicated optical transport to the experimental stations (ES1, 2, 3 in Fig. 1) for pump-probe experiments. The SL pulse generated by the OPA meets the electron bunch (represented by the yellow ellipse) and initiates the FEL process. The FEL pulse propagates in the undulator chain and through the X-ray beam transport optics, while the USL pulse propagates in parallel through its transport trajectory and, if the delay is properly chosen, arrives simultaneously with the FEL beam onto the sample under investigation.

Clearly, to get the full advantage of this scheme, the PPL beam optical transport from the seed laser room to the experimental stations should maintain a high pointing stability and keep the timing jitter between the propagated beam and the electron bunch as low as possible. For this reason, when applying this scheme at the FERMI FEL we paid special attention to both the mechanical and optical design, as well as to the active stabilization of the beam pointing. All these design aspects and data on the measured performance of the beam transport have already been discussed in details in a dedicated paper [8]. Here, we will briefly summarize them for the sake of better understanding the results reported later in this paper.

3. Seed laser system and optical beam transport

The seed pulse starts from a femtosecond Ti:Sapphire oscillator (Micra, Coherent) which is repetition rate locked to the reference timing signal distributed over the facility [14]. The main part of the oscillator output beam is amplified in a chirped-pulse regenerative amplifier-

#208592 - $15.00 USD Received 21 Mar 2014; revised 8 May 2014; accepted 8 May 2014; published 20 May 2014

single pass amplifier tandem, which delivers pulses with an energy of up to 7 mJ and duration about 100 fs.

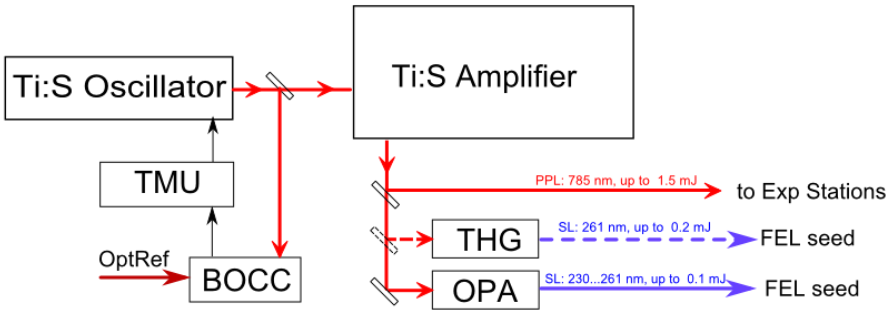

Fig. 2. Layout of the Seed Laser System.

As illustrated in Fig. 2, after leaving the Ti:Sapphire amplifier the IR pulse is split and about 70% of its energy is used to pump an OPA. The OPA is an infrared two-stage parametric amplifier (OPerA-Solo, Coherent). To obtain the needed UV seeding range, the OPA signal pulse is frequency-mixed with a fresh portion of the pump and then frequency doubled to get pulses with wavelength 228-261 nm and duration from 150 to 180 fs [15]. As it can be seen from the figure, it is also possible to seed the FEL directly with the third harmonic of the Ti:Sapphire amplifier, however, the experiments reported later in this paper have used only the OPA based seeding option.

In the other arm, the remaining IR pulse energy (typically about 1.2 mJ) propagates to the experimental stations along a total distance of about 150 m. Recalling that details can be found in ref [8], here we will only summarize the main results:

- The beam propagation to the beamlines preserves a very good beam quality, and introduces a slight positive chirp and pulse lengthening to about 120 fs due to material dispersion.
- Beam pointing stability when the active beam stabilization is ON is rather high, typically on the order a few micron RMS at the focal point of the last lens.
- The timing jitter introduced by the beam transport from the seed laser table to the optical breadboard of the DiProi station is below 3.6 fs RMS when the beam pointing feedback is ON.
- The Ti:Sapphire amplifier introduces a timing jitter of slightly less than 6 fs, which however will not contribute to the overall pump-probe jitter because this unit is common for both the SL and USL pulses.
- The OPA, which makes part of the SL pulse only, was found to also introduce a timing jitter of up to 6 fs during the measurements reported in [8]. For the experiments reported in the next chapter the OPA pump pointing was actively stabilized, so we expect the latter value is smaller. We think that it anyway remains the major contribution to the jitter values reported below.

4. Optical setup at the experimental stations

The USL pulse arrives in the experimental hall at a specially designed stable pillar from where it is distributed to the end-stations. Each end station has a dedicated optical breadboard where a number of important pulse manipulations/controls can be performed. Coarse and fine laser beam steering is obtained by using stepper motor-driven kinematic mounts and piezo tip-tilt platforms (PI S-330.20L), respectively. The fine steering is also used for beam

#208592 - $15.00 USD Received 21 Mar 2014; revised 8 May 2014; accepted 8 May 2014; published 20 May 2014

pointing stabilization, in combination with a real-time CCD-based beam position diagnostics. Two optical delay lines (coarse and fine delay) allow adjustment of the laser pulse arrival time at the sample. The fine delay can be scanned by about ± 650 ps using a retro-reflector mounted on 20 cm long translator stages. Each optical breadboard also contains a beam-size adjustment and focusing, as well as variable beam attenuation, performed by a λ/2 plate mounted on a remotely controlled rotation stage, and a pair of thin-film polarizers. In addition, a polarization control of the beam is implemented, allowing both adjustable linear and circular polarization to be set for the exit beam.

In this section we present two different experimental set-ups used to evaluate the arrival jitter inside the experimental end-stations of the FERMI user facility. The DiProI end-station (see Fig. 3(a)) adopts a non-collinear geometry between the FEL and the laser: the IR beam, focused by the lens L1, impinges on the sample at an angle of 45°, while the FEL beam arrives normal to the sample surface. The reflected IR beam is collected inside the chamber by the lens L2, which images the sample plane onto the CCD2 camera. In this non-collinear geometry the angle between the IR and the FEL pulse fronts leads to encoding of the time arrival information into the transverse (*x* axis) position along the sample [5,16]. In this way, if the sample reflectivity is modified by the pump pulse, the exact imaging of the reflected beam

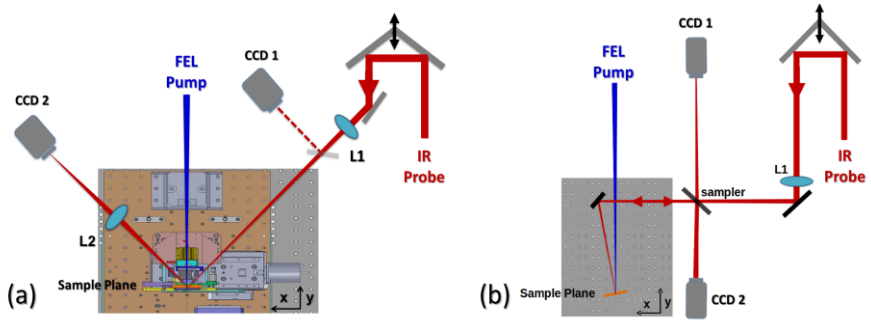

Fig. 3. Experimental layout for FEL pump – IR laser probe experiment, (a) at the DiProI end station and (b) at the Timex station.

distribution along the x-axis allows to extract the mutual position of the two pulses for each shot, provided their arrival time at the sample is within the time window determined by the beam dimension and the pulse tilt [4,5]. During the time resolved measurements of the FEL induced change of the optical constant, the FEL spot size inside the DiProI chamber was increased to ~250 μm FWHM using the active Kirckpatrick–Baez optical system of the beamline [17], while the IR laser was focused to ~125 μm spot size FWHM. The second scheme, adopted in the TIMEX end-station (see Fig. 3(b)), uses almost collinear geometry with negligible angle between the two pulse fronts. The delay between the two pulses is constant over the sample surface and is determined by the position of the fine delay stage. The USL beam is focused by a lens mounted outside the chamber and the back-reflected signal is monitored after a beam-splitter by CCD2. In this setup the FEL was focused to ~80 μm (FWHM) and the IR to ~70 μm (FWHM).

As a first step in both set-ups the coarse timing coincidence of the USL and FEL pulses was adjusted to a sub-50 ps level by using the signal generated on a specially designed copper antenna [17] connected through a high bandwidth coax cable to a fast oscilloscope (LeCroy SDA11000). Then, the fine delay was scanned, looking at the intensity of the IR pulse reflected by GaAs, Si, or Si_3N_4 sample. Figure 4(a) shows typical reflectivity traces obtained using the set-up in Fig. 3(a). The plotted reflectivity change ΔR/ R was calculated for each delay position by integrating the signal over the full CDD2 image for each shot with FEL ON with respect to the signal with FEL OFF. As it has already been reported in the literature previously [4,5,16,17] the electronic excitations induced by the FEL pulse lead to an abrupt

#208592 - $15.00 USD Received 21 Mar 2014; revised 8 May 2014; accepted 8 May 2014; published 20 May 2014

drop of the optical reflectivity occurring in the sub-ps time scale. A close inspection of the results obtained for Si_3N_4, Si and GaAs (see Fig. 4(a)) shows that the initial reflectivity drop is faster for Si_3N_4 (~300 fs) compared to Si (~550 fs) and GaAs (~750 fs). The observed reflectivity change rates are determined by the convolution of the intrinsic electronic response time of the sample with the FEL pulse duration (~100 fs FWHM), the USL pulse duration (~130 fs FWHM) and an additional Gaussian term taking into account the effective pulse lengthening due the tilted front geometry when the signal is integrated over the full image. As already observed previously, the reflectivity recovery from the fast initial drop occurs at longer time scales, depending on the band structure of the sample [18,19] and the recovery time of Si is considerably longer than that of GaAs (~4ps) and Si_3N_4 (~700 fs). The traces shown on Fig. 4(a) clearly indicate that Si_3N_4 is the best choice for the accurate measurement of the arrival time jitter between FEL and USL pulses due to the faster reflectivity change. Similar reflectivity measurements have been performed also at the TIMEX experimental station with the setup sketched on Fig. 3(b). Figure 4(b) shows a typical trace for a Si_3N_4 sample, pumped at 18.8 nm. As it can be seen, in this case the leading edge of the observed transient reflectivity change is faster, about 150 fs, which can be attributed to the nearly collinear geometry, i.e. the absence of pulse front tilt effect.

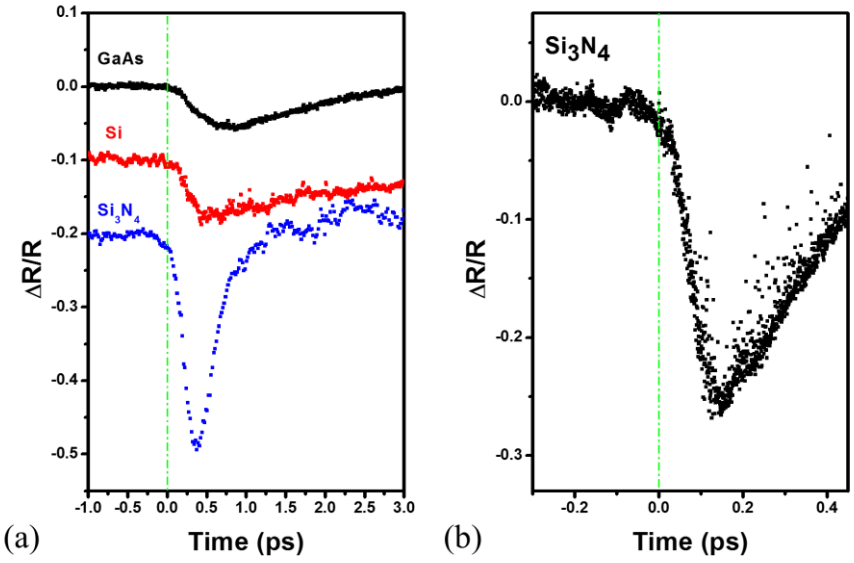

Fig. 4. (a) Reflectivity changes in GaAs, Si and Si_3N_4 samples induced by FEL pulses at 32.5 nm, measured on DiProi experimental station (see set-up on Fig. 3(a)); (b) Reflectivity changes in Si_3N_4 induced by FEL pulses at 18.8 nm, measured on the TIMEX experimental station (see set-up on Fig. 3(b)). The FEL pulse fluence was in the range 10 - 20 mJ/cm^2, while the one of the USL pulse was kept below 5 mJ/cm^2. The position of the delay stage for which the onset of the variation of IR reflectivity is observed, has been chosen, consistently for all measurements, as the origin of the time axis.

Also, the FEL pulses at 18.8 nm are expected to be shorter than the ones at 32.5 nm (by about 25%) due to the fact that the FEL was operating at a higher harmonic number. It is worth noting that Fig. 4 shows the raw data without any correction for the pulse arrival time or FEL intensity fluctuations. Using a Si_3N_4 target we performed a set of experiments aimed at quantifying the jitter with a measurement procedure as follows. (i) several scans of the pulse delay were made in order to calibrate the reflectivity change in the fast slope vs pump/probe time delay; (ii) the pump-probe delay was set at the middle of the fast reflectivity change slope; (iii) the reflected beam intensity, integrated over the CCD detector, is acquired for a few thousand shots. In order to correlate the experimental data, the FEL intensity was also recorded shot-by-shot using the FERMI online ionization chamber as intensity monitor.

#208592 - $15.00 USD Received 21 Mar 2014; revised 8 May 2014; accepted 8 May 2014; published 20 May 2014

Figure 5 shows typical data sets of timing fluctuations for the two end-stations. The statistical analysis of the recorded arrival time fluctuation, after filtering the FEL intensity in the range of ± 15% around the mean value, shows a jitter level of about 9.8 fs (RMS) for DiProI end station (Fig. 5(b)) and 5.9 fs for the TIMEX one (Fig. 5(d)). It is seen that for both experimental set-ups the measured timing jitter is significantly smaller than the best value of FEL-USL jitter reported in the literature (33 fs RMS in ref [7].). Measurements lasting longer (e.g. more than 20 min) were also performed at both end-stations, confirming that the slow timing drifts were negligible over tens of minutes. Moreover, two scans performed at DiProI on the same sample with a time interval of about 24 hours showed a shift of the pump-probe 'zero' time of only 65 fs.

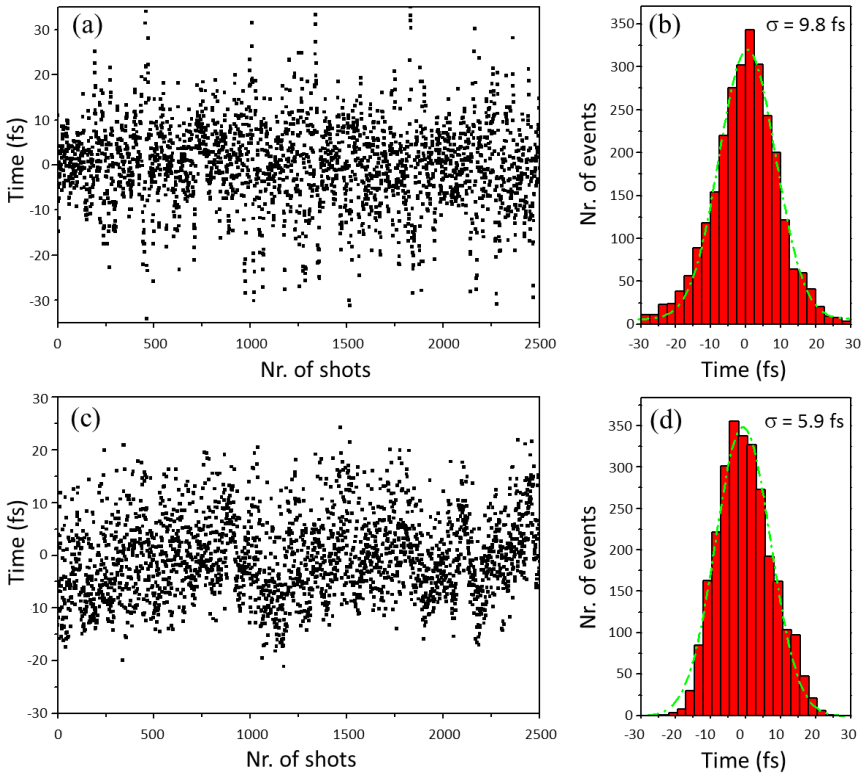

Fig. 5. A sequence (left) and histogram (right) of the relative timing of 2500 consecutive FEL and IR laser shots at the DiProI (a)-(b) and TIMEX end stations (c)-(d). The calibration needed to convert the intensity fluctuations measured by the detector to jitter arrival time between FEL (pump) and IR (probe) pulses was done by performing several time-delay scans in the region of the transient reflectivity signal as shown in Fig. 4. Then, the average slope of the fast reflectivity drop of Si_3N_4 was evaluated and used for obtaining the time scale of this figure.

As already explained above, the non-collinear pump-probe geometry sketched in Fig. 3(a) is suitable for performing single shot measurements, where the time evolution of the sample reflectivity is obtained by decoding the transverse modulation of the acquired images. Figures 6 and 7 illustrate that the instant when the FEL pulse hits the Si_3N_4 sample is visualized by the IR beam image. The image in Fig. 6(a) is obtained with a time delay tuned in a way that the FEL pulse arrives close to the center of the time window. In Fig. 6(b), the horizontal profile of this image is displayed in red, the black curve shows the image profile with FEL pulse OFF, while the green is the difference of the two profiles, i.e. the transient reflectivity trace. The single shot scheme allows the FEL-USL laser timing jitter measurement by observing the fluctuation of the position of the leading edge of the consecutive images taken

#208592 - $15.00 USD Received 21 Mar 2014; revised 8 May 2014; accepted 8 May 2014; published 20 May 2014

at a fixed delay. Figure 6(c) shows a sequence of 700 shots were the leading edge is indicated by the blue arrow. Performing a statistical analysis of the fluctuation a timing jitter of 9.5 fs in RMS is calculated (Fig. 6(d)), a value which is in excellent agreement with that obtained using the approach based on scanning. We note that in this last jitter estimation the effect of the non-uniformity of the FEL pump beam is not taken into account. We estimated that in our irradiation and jitter conditions the deformation of the measured reflectivity (green) curve in Fig. 6(b) due to the slightly different pump intensity seen by the probe at different time delay may lead to an uncertainty in the time delay determination of less than 2 fs. If this setup is used for shot-to-shot timing measurement aimed at post-processing data correction [16] and in conditions of larger pump-to-probe jitter the effect of pump non-uniformity may need to be precisely calculated. We also attached a video with a real time acquisition containing all images acquired in 10 seconds by CCD2 (a single frame is shown on Fig. 7), where one can appreciate the high stability of the setup (note that there is no any filtering or correction for the FEL intensity fluctuations).

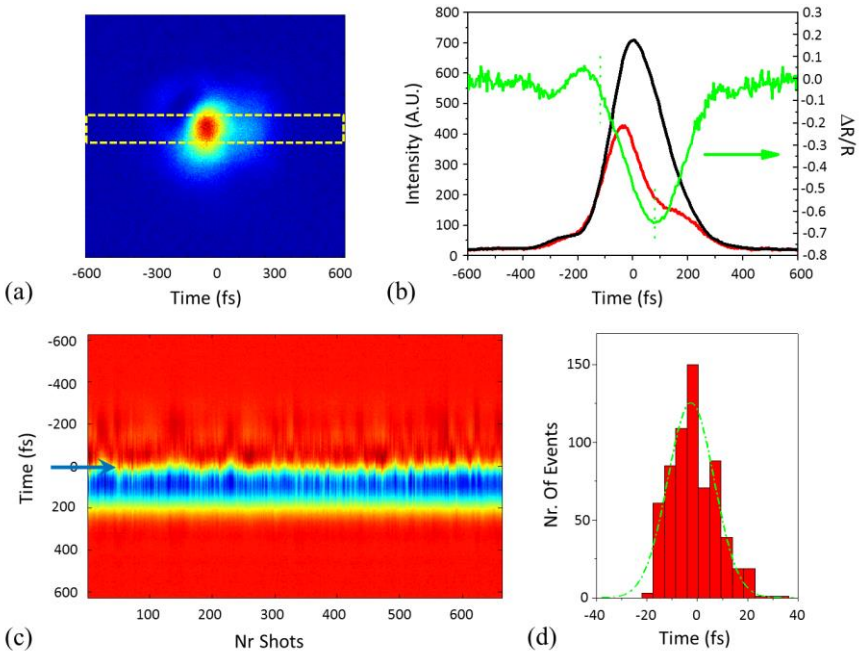

Fig. 6. **(**a) Image of the IR beam reflected by the Si_3N_4 sample when the FEL pulse arrives slightly after the IR pulse. (b) Red curve: IR beam image profile taken along the zone marked with a dashed yellow line in (a); black curve is the image of the same zone with FEL OFF; green curve: calculated local reflectivity variation on the sample plane, the vertical dash-dot lines mark the leading edge used in the jitter analysis. (c) Sequence of 700 consecutives FEL shots, the blue arrow indicates the shot-to-shot jitter fluctuation. (d) Histogram of the measured jitter fluctuation.

#208592 - $15.00 USD Received 21 Mar 2014; revised 8 May 2014; accepted 8 May 2014; published 20 May 2014

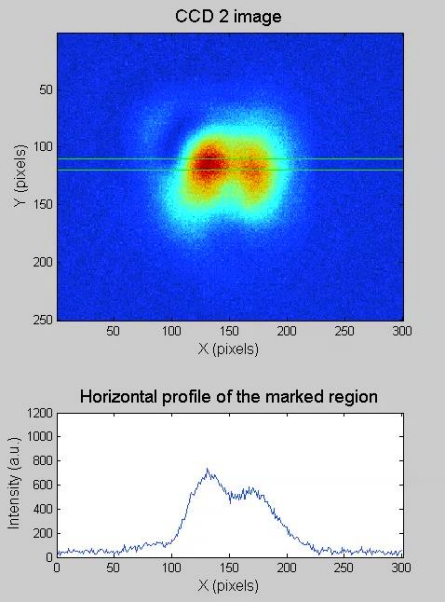

Fig. 7. An image extracted from the video showing the shot-by-shot behavior of the IR beam shape. The 'hole' position visualizes the arrival of the FEL pulse (see also Media 1).

5. Conclusions and outlook

The timing stability values reported in the present paper clearly demonstrate that our method drastically reduces the FEL-USL jitter and allow reaching values that are significantly lower than the ones presently achievable by the standard scheme. We believe that there are relatively straightforward routes to further improvements.

In this respect we note that in our scheme the precise feedback control of the IR laser beam propagation has an important role. In fact, we observed that with the feedback switched OFF the timing fluctuations were typically increasing by a factor of two or more, depending on the external conditions. We note that so far only a relatively low bandwidth (≤1 Hz) beam pointing stabilization feedback could be applied, which was clearly not sufficient to fully cancel the influence of external noise. It can therefore be expected that the implementation of faster feedback loops (bandwidth increase by a factor of 5 is possible with the existing hardware and much more if CCDs are replaced by position sensitive detectors) would allow to compensate to a higher extent the beam-path fluctuations caused by vibrations and acoustic noise coming from the environment. As it has been shown in [8] and mentioned above, a major contribution to the total FEL-USL timing fluctuations in our scheme is the OPA which is present in the SL pulse part only. The means to reduce the OPA induced timing jitter are under investigation, we can anticipate that also here the implementation of a dedicated to the OPA higher bandwidth pump beam pointing stabilization, as well as improved vibration isolation, is expected to lead to a reduction of the timing jitter added by the OPA to few fs RMS level.

We also note the importance of the stability and good vibration and acoustic isolation of the final part of the optical transport, i.e. the optical setup at the end-station. In fact, the better jitter performance observed on TIMEX can be attributed to the special effort dedicated to address these aspects on the TIMEX optical breadboard.

In conclusion, using the advantages of the seeded-FELs, we were able to devise a setup allowing FEL-external laser pump-probe experiments with unprecedentedly low time jitter. Using measurements of FEL induced transient reflectivity changes of Si_3N_4 targets, probed by an external optical laser, we demonstrate timing jitter of less than 6 fs RMS between the

#208592 - $15.00 USD Received 21 Mar 2014; revised 8 May 2014; accepted 8 May 2014; published 20 May 2014

pump and probe pulses. This result paves the way towards experiments where the control on different pulses timing is fundamental to reach the frontier of the ultrafast timescales of electron motion around an atom, the spatial scale of the interatomic distance and the energy scale of chemical bonds. Once crossed these borders, one can get the very essence of chemistry and condensed matter physics, which will certainly impact the development of next technologies.

Acknowledgments

This work was performed in the framework of the FERMI@Elettra Project of Elettra Sincrotrone Trieste, and partially supported by the Italian Ministry of Education, Universities and Research (MIUR) under grants FIRB-RBAP06AWK3 and ELI. C. M. acknowledges support from the European Research Council through the ERC Grant N.202804–TIMER.